Fibre Bragg gratings fabrication in four core fibres

Changle Wang*[a], Zhijun Yan[a], Qizhen Sun[a, b], Zhongyuan Sun[a], Chengbo Mou[a], Junxi Zhang[a], Abdulyezir Badmos[a], Lin Zhang[a]
[a]Aston Institute of Photonic Technologies, Aston University, Birmingham B4 7ET, UK;
[b]School of Optical and Electronic Information, Huazhong University of Science and Technology, Wuhan 430074, China. *Corresponding author: wangc15@aston.ac.uk

ABSTRACT

Due to the limitation of the lens effect of the optical fibre and the inhomogeneity of the laser fluence on different cores, it is still challenging to controllably inscribe different fibre Bragg gratings (FBGs) in multicore fibres. In this article, we reported the FBG inscription in four core fibres (FCFs), whose cores are arranged in the corners of a square lattice. By investigating the influence of different inscription conditions during inscription, different results, such as simultaneous inscription of all cores, selectively inscription of individual or two cores, and even double scanning in perpendicular core couples by diagonal, are achieved. The phase mask scanning method, consisting of a 244nm Argon-ion frequency-doubled laser, air-bearing linear transfer stage and cylindrical lens and mirror setup, is used to precisely control the grating inscription in FCFs. The influence of three factors is systematically investigated to overcome the limitations, and they are the defocusing length between the cylindrical lens and the bare fibre, the rotation geometry of the fibre to the irritation beam, and the relative position of the fibre in the vertical direction of the laser beam.

Keywords: Multicore fibre, fibre Bragg grating, grating inscription

1. INTRODUCTION

Single mode fibre (SMF) based optical communication is approaching its fundamental capacity limits. Several techniques have been applied to increase the transmission capacity, such as polarization division multiplexing (PDM) and dense wavelength division multiplexing (DWDM), in tandem with advanced modulation formats and coherent transmission techniques. As an alternative technique, multicore fibres (MCFs) with multiple single-spatial-mode cores were initially proposed as the solutions of Space-division multiplexing (SDM) to unlock the capacity of current optical communication systems[1]. From the past, MCFs have also been attracting more and more interest in microwave photonics (MWP)[2], optical sensing[3, 4], "photonic lantern"[5], Raman amplification[6], pulse manipulation[7] etc.. As a matured technique to fabricate all fibre devices, UV inscribed optical fibre gratings have been intensively developed and applied in three main research areas, such as fibre communications, fibre lasers and fibre sensing area[8]. Recently some research groups have reported the fabrication and application of fibre Bragg gratings (FBGs) in MCFs applied in optical communications, MWP[9], optical sensing[10-15], photonic lantern[16], lasers and amplification[17, 18] etc..

Though the inscription of FBGs in all cores of MCF at the same position with similar characteristics is very important in both optical fibre communications and sensing, it is still challenging due to the limitation of the lens effect of the optical fibre and the inhomogeneity of the laser fluence on different cores. In this article, we will focus on the FBG inscription in four core fibres (FCFs), whose cores are arranged in the corners of a square lattice, at different inscription conditions to achieve simultaneous inscription of all cores, selectively inscription of individual or two cores, and even double scanning in perpendicular core couples by diagonal. The phase mask scanning method, consisting of a 244nm Argon-ion frequency-doubled laser, air-bearing linear transfer stage and cylindrical lens and mirror setup, is used to precisely control the grating inscription in FCFs. The influence of three factors is systematically investigated to overcome the limitations, and they are the defocusing length between the cylindrical lens and the bare fibre, the rotation geometry of the fibre to the irritation beam, and the relative position of the fibre in the vertical direction of the laser beam.

Micro-Structured and Specialty Optical Fibres IV, edited by Kyriacos Kalli, Alexis Mendez, Proc. of SPIE Vol. 9886, 98860H · © 2016 SPIE
CCC code: 0277-786X/16/$18 · doi: 10.1117/12.2227040

2. FABRICATION AND CHARACTERISATION OF FBG IN MCF

In our experiment, two different commercial homogeneous FCFs, provided by *Fibercore Ltd.*, are used for FBG fabrication, one with normal communications cores arranged in the corners of a 36-μm-side square lattice, the other with Germanium and Boron co-doped highly photosensitive cores arranged in the corners of a 50-μm-side square lattice. The diameter of the fibre and the cores are 125 μm and 8 μm for both FCFs. The normal crosstalk level is less than −25 dB to avoid significant transmission penalties for signals around C band[19] and both types meet the limit level well. Fig.1 shows the measured cross-section and longitudinal images of both 36 μm and 50 μm core distance FCF under a 100x objective lens.

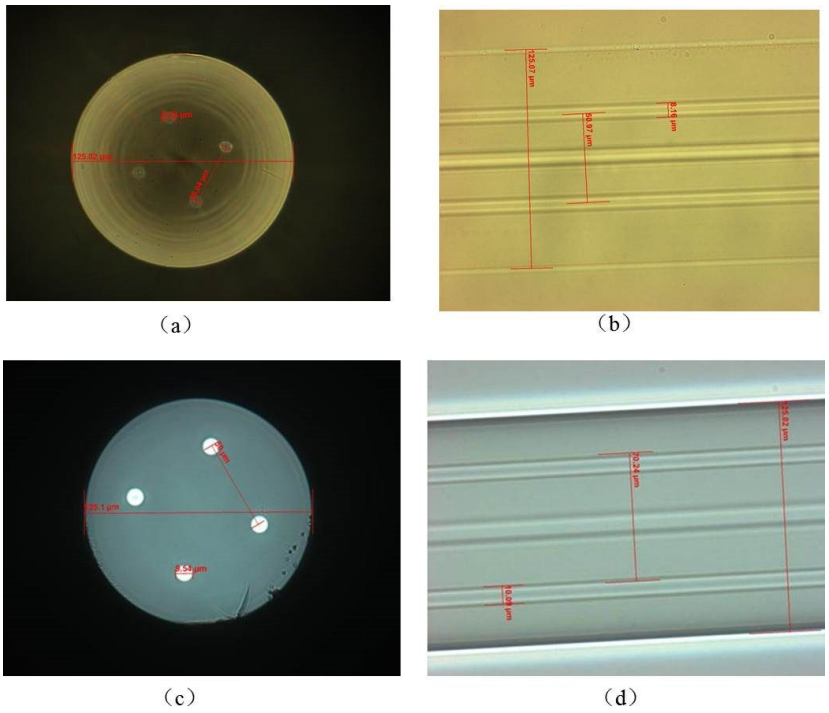

Figure 1 Microscopic images of cross-section (a) and longitudinal (b) for 36 μm FCF, cross-section (c) and longitudinal (d) for 50 μm FCF

The 36μm core distance FCFs have been designed for high capacity optical communications and hold no photosensitivity. So hydrogenation process is necessary to increase the photosensitivity before the FBG inscription. During the hydrogenation process, fibres are treated in 150-bar pressure H_2 chamber at 80°C temperature for 48 hours. While the Boron and Germanium (B-Ge) co-doped fibres have enough intrinsic photosensitivity to allow FBG inscription without hydrogenation. In order to precisely control the grating inscription in the FCFs, we use phase mask scanning method to inscribe FBG. The grating fabrication system consists of a 244nm Argon-ion frequency-doubled laser, air-bearing linear transfer stage and lens and mirror setup (see Fig. 2). During the FBG fabrication in FCFs, the UV beam is firstly focused by a 87mm focus length cylindrical lens and goes through the standard phase mask on.

In the experiment, different inscription parameters, such as the laser power after phase mask, scanning velocity and grating length, have been applied to control the FBG inscription. The distance between the cylindrical lens and the bare fibre, the rotation geometry of the fibre to the irritation beam, and the relative position of the fibre core in the vertical direction of the laser beam are the three major controlling factors in order to achieve different types of abovementioned FBG inscription. The uniform phase mask from Ibsen Ltd. used for FCFBG inscription possessing 5 different periods (Λpm1=1.06085 μm, Λpm2=1.06639 μm, Λpm3=1.07192 μm, Λpm4=1.07745 μm and Λpm5=1.08298 μm), corresponding to resonance wavelength at 1535.9 nm, 1543.7 nm, 1551.7 nm, 1559.6 nm and 1567.6 nm, respectively. Because the 50 μm core distance FCF is specially fabricated for optical sensing and is far more expensive, most FCFs we have used are the commercial optical communication FCFs (with 36 μm core distance) unless introduced in advance.

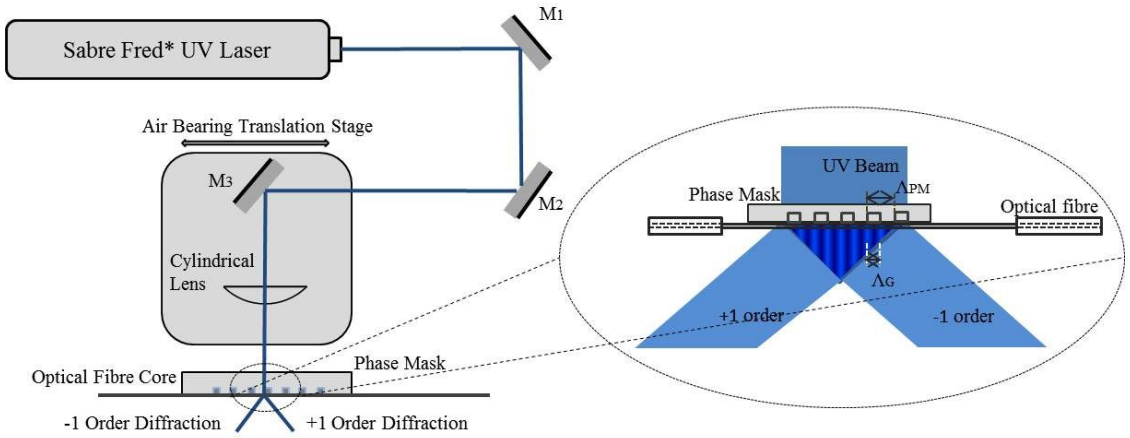

Figure 2 Schematic description of the phase mask scanning inscription system in our lab.

2.1 Affection of Defocus in UV Inscription

The effective laser beam size before cylindrical lens is approximately 450 µm measured by a UV beam profiler and it will be focused to around 22µm at the focus point, 87mm after the lens. Firstly the cylindrical lens is set to be 87 mm (d_1) distant from the FCF core, and then the laser beam with a 29mW output after mask scanned the fibre centre (Δf_1=0) through the Λ_{pm3} period mask area at a velocity of 0.04mm/s over a 6 mm length of fibre, as is shown in Fig. 3 (a). From the measured transmission spectra in Fig. 3 (b), it can be seen that only core C and core D in the beam axis are UV processed for FBG inscription. The measured central wavelength and transmission of the FBG in core C and core D are 1554.20 nm, -38 dB and 1553.99 nm, -27 dB respectively. During the UV irritation, core C experience UV exposure first and the core D lies partly in the shadow of core C, thus gets less UV exposure, which results in a shorter wavelength ($\Delta\lambda$=0.21 nm) and weaker reflectivity (ΔT=11 dB) compared to FBG inscribed in core C.

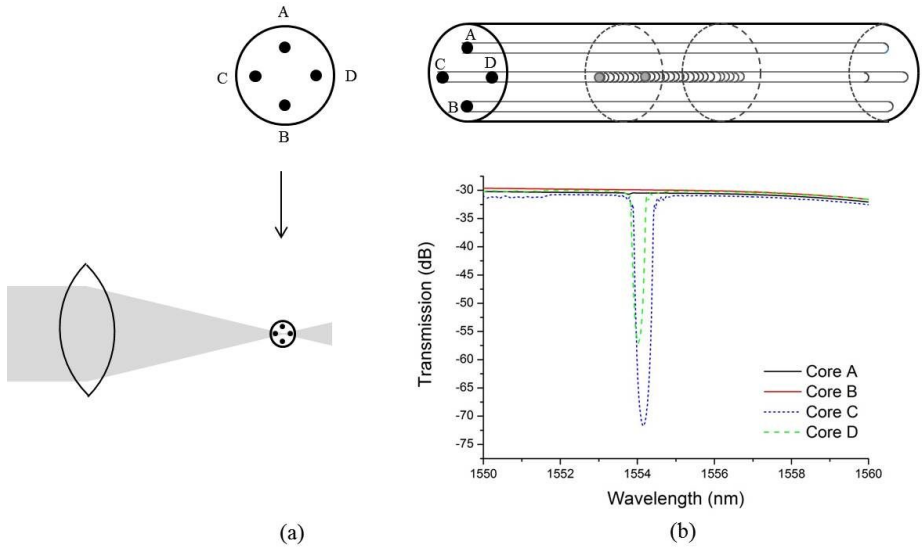

Figure 3 (a) Schematic diagram of FBG inscription in a FCF located at the lens' focus point; (b) transmission spectrum of all four cores.

In order to investigate the influence of the defocus length, the cylindrical lens is moved backwards by 3.5 mm (Δf_2) and 7.0 mm (Δf_3), corresponding to d_2=90.5 mm and d_3=94.0 mm. According to the measured results in Fig. 4 and 5, the vertical beam size almost doubles from 22.15µm (Δf_1=0), 48.21µm (Δf_2=3.5mm), to 96.48µm (Δf_3=7.0mm), while the horizontal beam size shrinks a little 806.47µm, 787.01µm, to 737.25 µm correspondingly.

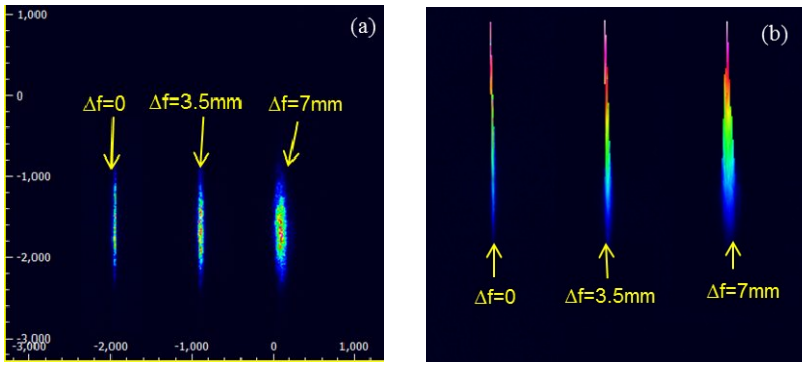

Figure 4 2D (a) and 3D (b) image of UV beam when Δf=0, Δf=3.5mm and Δf=7.0mm

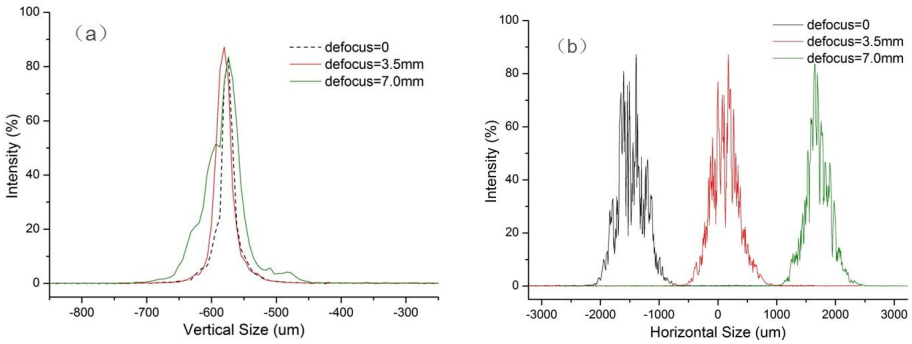

Figure 5 Measured beam size in vertical (a) and horizontal directions (b) when Δf=0, Δf=3.5mm and Δf=7.0mm

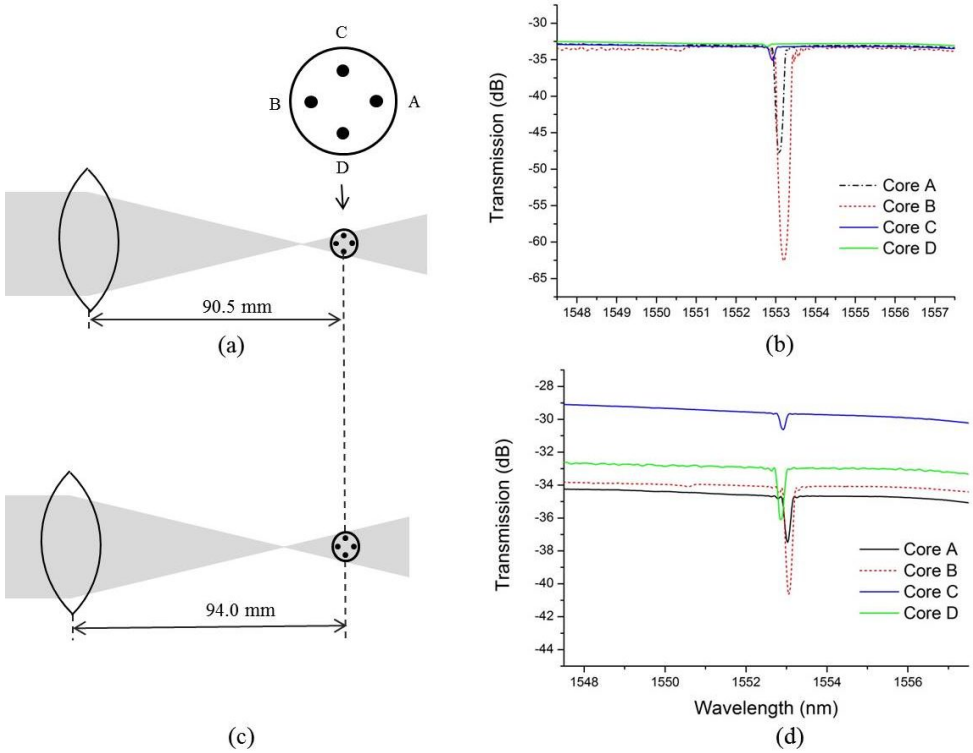

Figure 6 (a), (c) Schematic setup of FBG inscription under different focus conditions: Δf_2=3.5 mm and Δf_3=7.0 mm; (b) and (d) corresponding transmission spectra to Δf_2 and Δf_3 in four cores.

Table 1 Central wavelength and transmission dip distribution of the FBGs in four cores when inscribed with different defocus lengths (corresponding to Fig. 3 and 6).

Core	Δf_1=0		Δf_2=3.5mm		Δf_3=7.0 mm	
	λ/nm	Strength/dB	λ/nm	Strength/dB	λ/nm	Strength/dB
A	--	--	1552.95	15.3	1553.03	3.2
B	--	--	1553.25	29.5	1553.06	6.5
C	1554.20	38	1552.94	2.5	1552.92	1.1
D	1553.99	27	1552.92	0.6	1552.86	3.6

2.2 Simultaneous inscription in all cores

Given the limited Gaussian beam size and effective power distribution in the beam cross-section, the core to core distance perpendicular to the laser axis is desired to be as small as possible in order to balance the decreasing lower laser fluence with the increasing defocus distance. The fibre orientation during UV irritation is set as shown in Fig. 7 (a).

The inscription is accomplished with a velocity of 0.10mm/s over 5.0mm length at a 25mW laser power after mask. The inscription of the same orientation with a 50μm core distance FCF is illustrated in Fig. 8 (a) with a same velocity and laser power but over a 10mm length. From Table 2, we can get $\Delta\lambda_{M4}$ = 0.16nm, RT_4 = 3.0dB and $\Delta\lambda_{M5}$ = 0.54nm, RT_5 = 12dB. Obviously the wavelength and strength uniformity has been improved significantly. Besides, the 50μm core distance FCF has shown a higher intrinsic photosensitivity than the 36μm core distance FCF with hydrogenation even considering the twice exposure grating length.

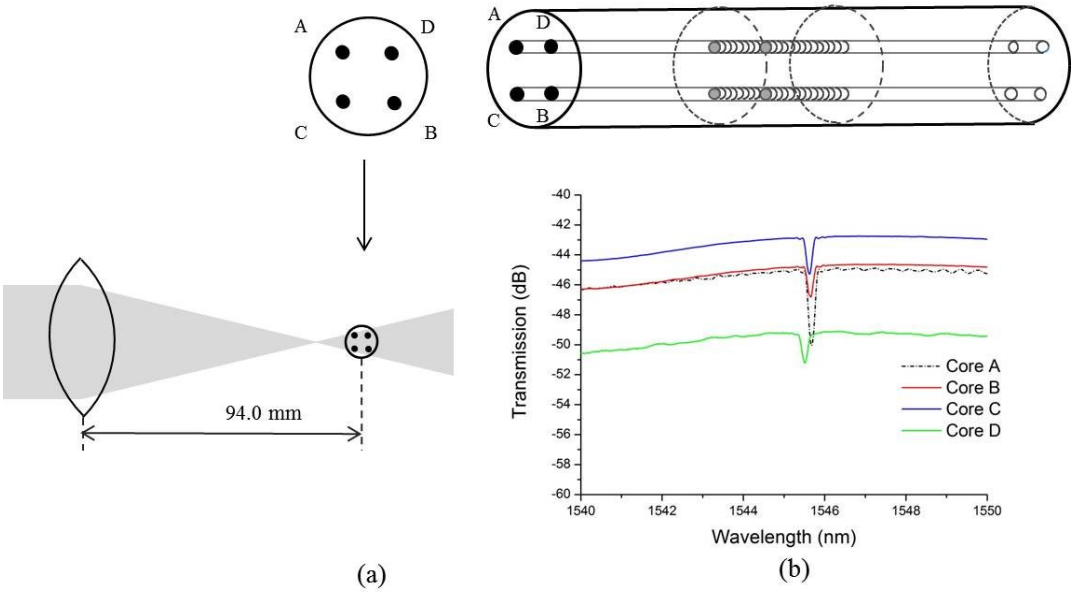

Figure 7 (a) Schematic setup of FBG inscription with Δf_4=7.0 mm in 36μm FCF; (b) corresponding transmission spectra.

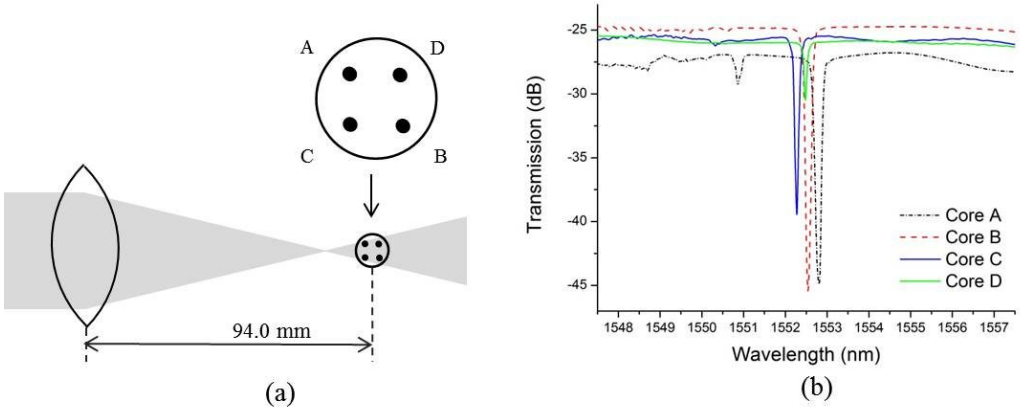

Figure 8 (a) Schematic setup of FBG inscription with Δf_5=7.0 mm in 50μm core distance FCF; (b) corresponding transmission spectra.

Table 2 Central wavelength and transmission dip distribution of FBGs in two different kinds of FCF inscribed with a rotated orientation (corresponding to Fig. 7 and 8).

Core	36μm FCF, Λ_{pm2}=1.06639 μm		50μm FCF, Λ_{pm3}=1.07192 μm	
	λ/nm	Strength/dB	λ/nm	Strength/dB
A	1545.68	5.0	1552.81	18.5
B	1545.63	2.0	1552.54	20.5
C	1545.63	2.5	1552.27	13.8
D	1545.52	2.0	1552.46	6.5

2.3 Single core inscription

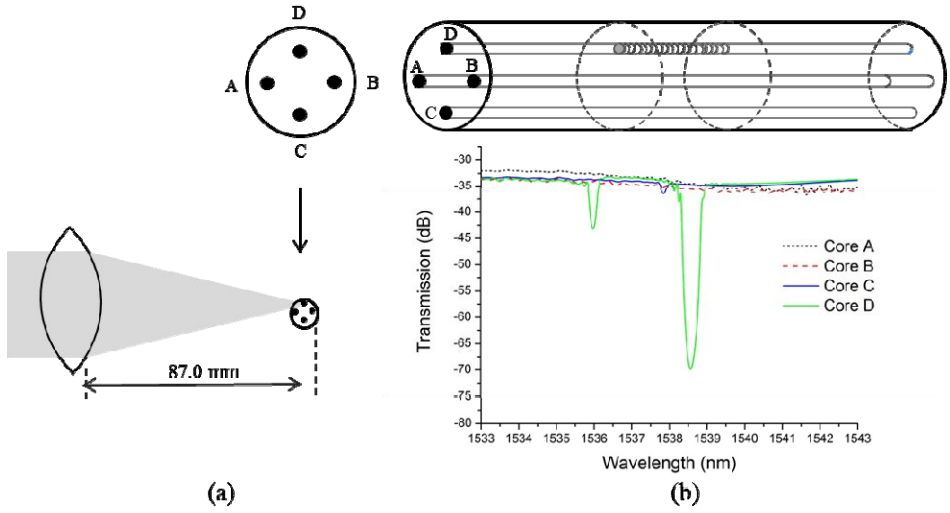

Figure 9 (a) Schematic setup of single core FBG inscription when Δf_6=0 in 36μm FCF; (b) corresponding transmission spectra.

In some cases, independent inscription of selective core or cores of the MCF is necessary, i.e. selectively writing with uniform FBGs and linearly chirped FBGs (LC-FBG) for MWP[9]. For this purpose, a third experiment is performed to

study the FBG inscription in a single core, as shown in Fig. 9 (a). A 70mW laser beam is scanned through the Λ_{pm1}=1.06085μm mask area at 0.05mm/s velocity over a length of 5mm. According to the corresponding spectra response in Fig. 9 (b), only core D is mainly inscribed with response wavelength at 1538.66nm and 37dB. No obvious spectral response for both core A and core B. This proves the effectiveness of our individual core inscription. However, due to the limited focused beam size, we are still able to see FBG inscribed in core C with the measured central wavelength and reflectivity of 1537.88nm and 1.5dB respectively. Moreover, the same alignment inscription is used for the 50μm core distance FCF as Fig. 10 illustrates. Similarly, only core D is inscribed with 1561.01nm wavelength and 15.20dB depth.

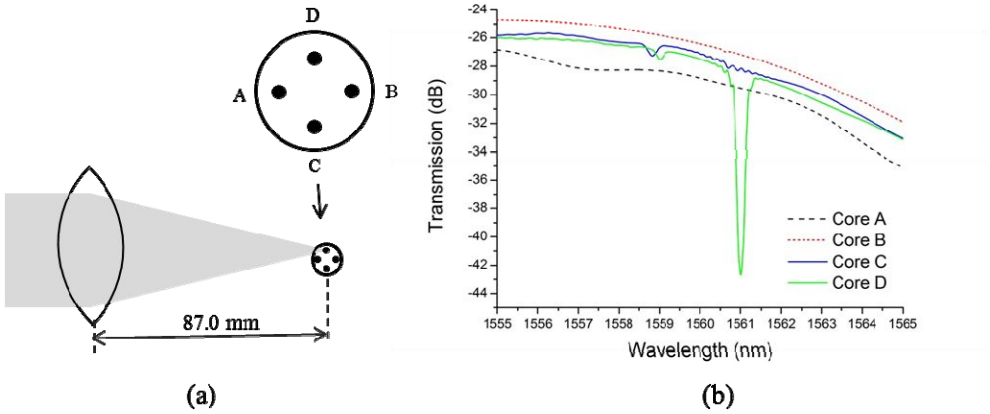

Figure 10 (a) Schematic setup of single core FBG inscription when Δf_7=0 in 50 μm core distance FCF; (b) corresponding transmission spectra.

2.4 Double scanning inscription

All the above FBGs in different FCFs have been inscribed simultaneously at the same position, which can be named "single scanning inscription". In order to inscribe FBGs in all cores at the same position with uniform spectra response more effectively, another approach based on inscription setup like Fig. 3 with Δf=0 has been proposed, which is "double scanning inscription". In the double scanning inscription, when the first scanning finishes, the fibre will be rotated by 90° to have the other perpendicular core couple irritated. Two experiments in this method are carried out and the corresponding spectral responses are shown in Fig. 11.

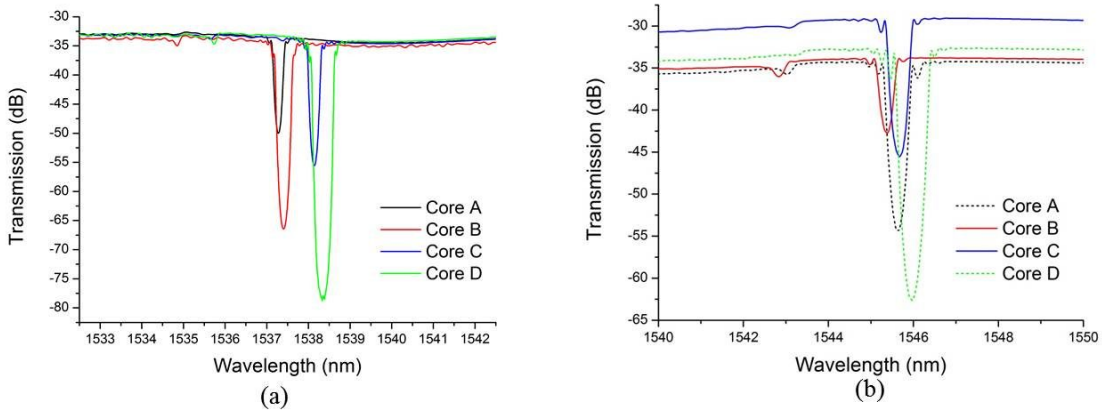

Figure 11 Transmission spectra response by double scanning inscription with different mask (a) Λ_{pm1}=1.06085μm and (b) Λ_{pm2}=1.06639 μm

Table 3 Central wavelength and transmission dip distribution of FBGs in two wavelength area by the double scanning method (corresponding to Fig. 11).

Core	Δf_8=0, Λ_{pm1}=1.06085 μm		Δf_9=0, Λ_{pm2}=1.06639 μm	
	λ/nm	Strength/dB	λ/nm	Strength/dB
A	1537.25	16	1545.64	20.5
B	1537.36	32	1545.39	8
C	1538.00	20	1545.67	16
D	1538.33	45	1545.98	30

According to Table 3 and Figure 8, we can see that during the scanning in the same time the former one of the core couple lying in the beam axis always experiences stronger exposure and leads to a higher reflectivity (twice than the following one) and longer resonance wavelength. While the wavelength difference between two scanning is relatively large, and it can be accounted to the strain fluctuation during rotation by 90°.

In light of the above FBG inscription and spectral measurement, different factors (including the defocus length, orientation of the fibre core, and relative position between the laser beam and the fibre centre), have been investigated in the FBG inscription in order to get the FBGs in all cores, a core couple or a single core. Moreover, double scanning inscription is also implemented to get all 4 cores inscribed at the same wavelength.

3. CONCLUSION

In this article, the inscription of different FBG groups in two types of FCF is studied. The influence of defocus length, the geometry and arrangement of FCF, and the relative position between laser beam and fibre core are investigated. For a four core fibre whose cores are distributed in the corners of a square lattice, FBGs has been inscribed in the diagonal direction cores by putting the fibre at the focus point, and a single core inscription has also been achieved by mismatching the FCF centre slightly at the perpendicular direction of the laser beam. Through adjusting the defocusing length from Δf=3.5mm to Δf=3.5mm and Δf=7.0mm, all the four cores are irradiated by the UV laser and simultaneously inscribed with FBGs. Meanwhile, it is also important to rotate the FCF appropriately to make sure the back cores not lying in the beam shadow of the front cores. The central wavelengths and strength of the different core FBGs are investigated. In order to get the most efficient inscription of FBGs in all cores, the double scanning method is also tested, however, it brings about the wavelength shift due to the unavoidable strain effect.

In actual industrial applications, the number of FBGs in sensing system limits the interval spectral spacing, in order to avoid the interference of the side-lobes with the neighbour FBG spectra and the accompanying erroneous Bragg wavelength determination. Then the apodisation of FBG spectra in FCF can be of great value to enhance the spectral efficiency especially when using shorter FBGs with a broader FWHM. In order to better control the inscription of different FBG groups in MCF, the beam size compensation is desirable to eliminate the effect of beam fluence. The polished capillary tube, the relative arrangement of cores, modification of core geometry and photosensitivity balance, are all viable for a better simultaneous grating writing in the future work.

ACKNOWLEDGEMENT

This work was funded by UK EPSRC Program Grant UNLOC EP/J017582/1 and the European Commission's Marie Curie International Incoming fellowship 328263.

REFERENCE

[1] R. J. Essiambre, R. Ryf, N. K. Fontaine *et al.*, "Breakthroughs in Photonics 2012: Space-Division Multiplexing in Multimode and Multicore Fibres for High-Capacity Optical Communication," *IEEE Photonics Journal,* vol. 5, no. 2, pp. 0701307-0701307, 2013.

[2] I. Gasulla, and J. Capmany, "Microwave Photonics Applications of Multicore Fibres," *IEEE Photonics Journal,* vol. 4, no. 3, pp. 877-888, 2012.

[3] J. P. Moore, and M. D. Rogge, "Shape sensing using multi-core fibre optic cable and parametric curve solutions," *Optics Express,* vol. 20, no. 3, pp. 2967-2973, 2012.

[4] H. J. Lee, H. S. Moon, S. K. Choi *et al.*, "Multi-core fibre interferometer using spatial light modulators for measurement of the inter-core group index differences," *Optics Express,* vol. 23, no. 10, pp. 12555-61, May 18, 2015.

[5] T. A. Birks, B. J. Mangan, A. Díez *et al.*, "Photonic lantern spectral filters in multi-core fibre," *Optics Express,* vol. 20, no. 13, pp. 13996-14008, 2012.

[6] K. Suzuki, H. Ono, T. Mizuno *et al.*, "Pump Light Source for Distributed Raman Amplification in MCFs With LD Sharing Circuit," *IEEE Photonics Technology Letters,* vol. 24, no. 21, pp. 1937-1940, 2012.

[7] A. M. Rubenchik, I. S. Chekhovskoy, M. P. Fedoruk *et al.*, "Nonlinear pulse combining and pulse compression in multi-core fibres," *Optics Letters,* vol. 40, no. 5, pp. 721-4, Mar 1, 2015.

[8] K. O. Hill, and G. Meltz, "Fibre Bragg grating technology fundamentals and overview," *Journal of Lightwave Technology,* vol. 15, no. 8, pp. 1263-1276, Aug, 1997.

[9] I. Gasulla, D. Barrera, and S. Sales, "Microwave Photonic Devices Based on Multicore Fibres," in International Conference on Transparent Optical Networks, 2014, pp. 1-4.

[10] M. Silva-Lopez, C. Li, W. N. MacPherson *et al.*, "Differential birefringence in Bragg gratings in multicore fibre under transverse stress," *Optics Letters,* vol. 29, no. 19, pp. 2225-2227, 2004.

[11] M. J. Gander, W. N. Macpherson, R. McBride *et al.*, "Bend measurement using Bragg gratings in multicore fibre," *Electronics Letters,* vol. 36, no. 2, pp. 120-121, 2000.

[12] G. M. H. Flockhart, W. N. MacPherson, J. S. Barton *et al.*, "Two-axis bend measurement with Bragg gratings in multicore optical fibre," *Optics Letters,* vol. 28, no. 6, pp. 387-389, 2003.

[13] D. Barrera, I. Gasulla, and S. Sales, "Multipoint Two-Dimensional Curvature Optical Fibre Sensor Based on a Nontwisted Homogeneous Four-Core Fibre," *Journal of Lightwave Technology,* vol. 33, no. 12, pp. 2445-2450, 2015.

[14] A. Fender, E. J. Rigg, R. R. J. Maier *et al.*, "Dynamic two-axis curvature measurement using multicore fibre Bragg gratings interrogated by arrayed waveguide gratings," *Applied Optics,* vol. 45, no. 36, pp. 9041-9048, 2006.

[15] S. Dochow, I. Latka, M. Becker *et al.*, "Multicore fibre with integrated fibre Bragg gratings for background-free Raman sensing," *Optics Express,* vol. 20, no. 18, pp. 20156-20169, 2012.

[16] E. Lindley, S. S. Min, S. Leon-Saval *et al.*, "Demonstration of uniform multicore fibre Bragg gratings," *Opt Express,* vol. 22, no. 25, pp. 31575-31581, Dec 15, 2014.

[17] A. M. Rocha, T. Almeida, R. N. Nogueira *et al.*, "Analysis of power transfer on multicore fibres with long-period gratings," *Optics Letters,* vol. 40, no. 2, pp. 292-295, Jan 15, 2015.

[18] F. Y. M. Chan, and K. Yasumoto, "Design of wavelength tunable long-period grating couplers based on asymmetric nonlinear dual-core fibres," *Optics Letters,* vol. 32, no. 23, pp. 3376-3378, 2007.

[19] P. J. Winzer, A. H. Gnauck, A. Konczykowska *et al.*, "Penalties from In-Band Crosstalk for Advanced Optical Modulation Formats," in European Conference on Optical Communications, 2011, pp. 1-3.